Step-by-Step Self-Assembly of a Double-Walled Knotted Cage With Increasing Topological Complexity

Hiroki Takezawa,*[a] Yukari Tamura,[a] and Makoto Fujita*[b, c]

The self-assembly process of a double-walled cage formed from a semiflexible tripodal ligand and a Pd(II) 90-degree block was tracked by NMR and x-ray analysis. At least two intermediate structures with distinct topologies were observed prior to the formation of the final double-walled cage. By optimizing the self-assembly conditions (e.g., time, solvent, and concentration), these topological intermediates were successfully isolated and analyzed by x-ray crystallography. They are considered crucial metastable structures that navigate the shortest pathway to the final structure, demonstrating the critical role of molecular topology in guiding and controlling the kinetics of metal-directed self-assembly.

1. Introduction

In the self-assembly of well-defined complex structures, dynamic phenomena in which their frameworks change over time can generate a chemical system that exhibits time-dependent multifunctionality.[1] Recently, such dynamic behavior has also been reported in the self-assembly processes of molecular cages.[2] However, in conventional simple metal–ligand self-assemblies, the intermediate products formed on the way to the final product often possess similar kinetic and thermodynamic stabilities. As a result, they are observed as complex mixtures that change over time, making it difficult to identify their individual structures.[3]

On the other hand, when the assembly processes involve topological transformations (i.e., changes in the crossing number of molecular strands), the processes are thought to require significant motions, such as threading molecular strands through cyclic or looped frameworks, and thus tend to proceed relatively slowly.[4] In this study, we demonstrated that in the double-walled knotted cage **1**,[5] assembled from semiflexible ligand **2** and Pd(II) 90° block **3**, two well-defined interlocked isomers are stepwise formed prior to the final structure (Figure 1). These interlocked structures exhibited significantly different kinetic stabilities due to their topological differences, and it was confirmed that each product can be obtained in nearly pure forms in the order of increasing crossing numbers. This strategy reveals the critical role of topology in determining the kinetics and pathways of metal-directed self-assembly, offering valuable insights for designing controllable dynamic systems.

2. Results and Discussion

We previously reported double-walled knotted cage **1**, constructed from semiflexible ligand **2** and *cis*-endcapped Pd(II) complex **3**, with an $M_{12}L_8$ (M = metal, L = ligand) composition (Figure 1).[5] Here, we carefully tracked the initial stages of the self-assembled process (Figure 2). When a 2:3 mixture of ligand **2** and complex **3** in CD_3CN/D_2O = 1:4 ([**2**] = 10 mM) was stirred at room temperature for 10 min, a series of sharp ^1H NMR signals appeared along with broad signals that possibly derived from an oligomeric mixture (Figure 2b). The first NMR-identifiable product **4** has more than 30 aromatic signals, suggesting a lower symmetric structure. The product was then converted to another species 5 with much smaller numbers of signals upon heating at 100°C for 5 min (Figure 2c). Further reaction at 100°C for 1 day quantitatively gave cage **1** (Figure 2d).

Optimization of the self-assembly conditions allowed us to obtain each **4** and **5** in a nearly pure form. Stirring the reaction mixture in methanol-d_4 at room temperature for 10 min yielded complex **4** near quantitatively (Figure 2e). The ^1H NMR spectrum of the resulting solution revealed six distinct sets of signals corresponding to the ligand arms. This observation suggests the presence of two inequivalent ligands, each adopting three distinct orientations for their arms. The wide chemical shift range of aryl protons (4.7–10.2 ppm) indicated the formation of an interlocked structure, where shielding and deshielding effects

[a] H. Takezawa, Y. Tamura
Department of Applied Chemistry, School of Engineering, The University of Tokyo, Mitsui Link Lab Kashiwanoha 1, FS CREATION, 6-6-2 Kashiwanoha, Kashiwa, Chiba, Japan
E-mail: takezawa@appchem.t.u-tokyo.ac.jp

[b] M. Fujita
Tokyo College, UT Institutes for Advanced Study (UTAIS), The University of Tokyo, Mitsui Link Lab Kashiwanoha 1, FS CREATION, 6-6-2 Kashiwanoha, Kashiwa, Chiba, Japan
E-mail: mfujita@appchem.t.u-tokyo.ac.jp

[c] M. Fujita
Division of Advanced Molecular Science, Institute for Molecular Science (IMS), 5-1 Higashiyama, Myodaiji, Okazaki, Aichi, Japan

Supporting information for this article is available on the WWW under https://doi.org/10.1002/chem.202500009

Chemistry–A European Journal

Research Article
doi.org/10.1002/chem.202500009

Chemistry Europe
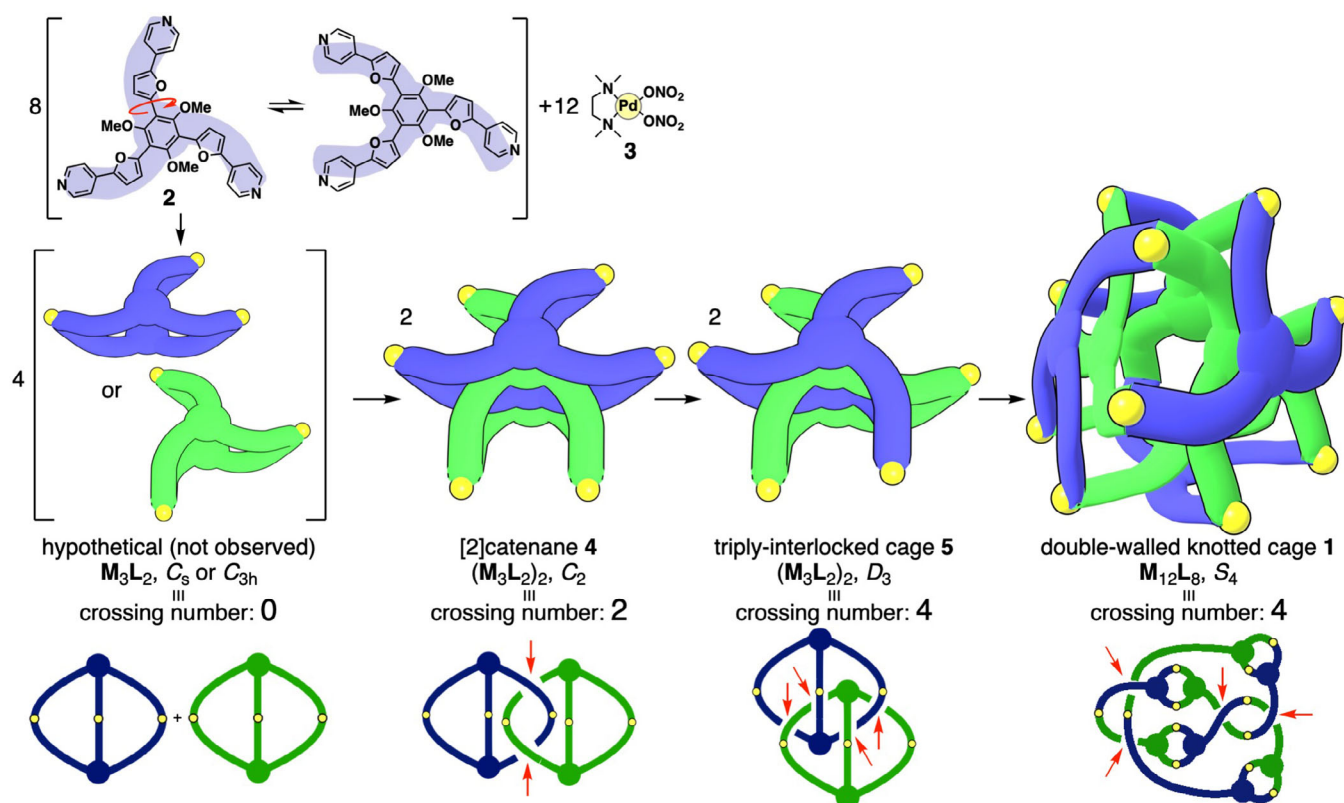European Chemical
Societies Publishing

Figure 1. Sequential formation of interlocked, double-walled complexes from a semiflexible ligand and a 90° Pd(II) block. The crossing number n indicates that the topology of a compound, regardless of how it is represented on a plane, will result in at least n crossings.
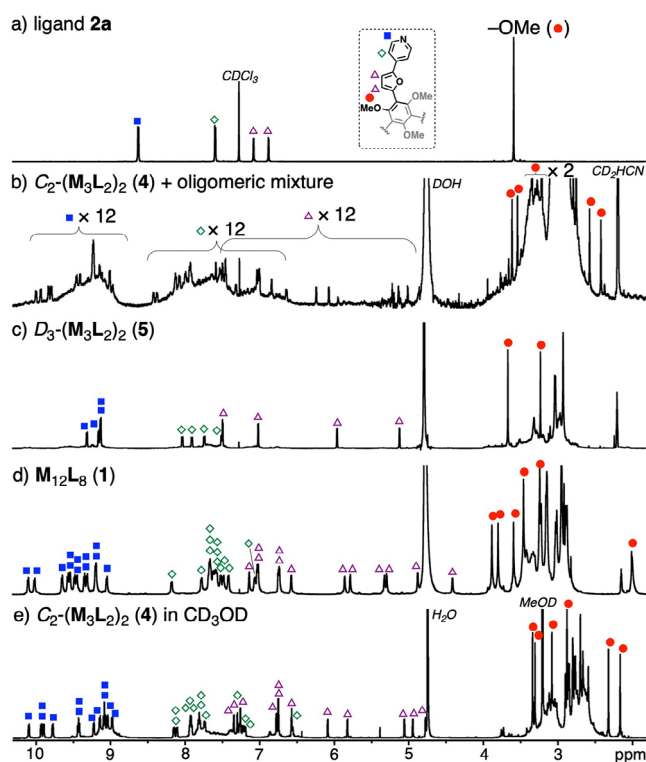

Figure 2. ^{1}H NMR spectra of (a) ligand **2** in CDCl$_3$, (b) a mixture after 10 min complexation at room temperature with **2** and **3** in CD$_3$CN/D$_2$O = 1:4, (c) complex **5** obtained after the complexation at 100°C for 5 min, (d) complex **1** in CD$_3$CN/D$_2$O = 1:4, and (e) complex **4** in CD$_3$OD.

arise from neighboring aromatic rings. In addition, ^{1}H DOSY NMR measurements revealed that all signals show the same diffusion coefficient (log$D = -9.5$, in CD$_3$OD), confirming the formation of a single, well-defined product **4** (Figure S8).

The structure of **4** was unambiguously determined through single-crystal x-ray diffraction using a synchrotron x-ray beamline (Figure 3a, see the Supporting Information for details).[6] Crystals suitable for the analysis were obtained by in situ anion exchange, replacing NO$_3^-$ with PF$_6^-$ by adding grains of KPF$_6$ salt to a methanol solution of **4**. By combining data from two crystals, we successfully resolved the crystal structure. Complex **4** adopts a *pseudo-C$_2$* symmetric structure comprising two interlocked, apparent C_s-symmetric M$_3$L$_2$ units. Each ligand in **4** exhibits a C_1 symmetric conformation, resulting in six virtually inequivalent ligand arms consistent with the NMR assignment. The kinetic product **4** possesses a [2]catenane topology,[7] which can also be described as a double-walled cage. The walls of the structure are formed by two non-symmetric, distorted ligands, similar in conformation to those observed in final knotted cage **1**. This feature highlights the propensity of the ligand to form a *pseudo*-hexapodal ligand by loose stacking interactions.

The second product, **5**, was obtained quantitatively by halting the assembly process after stirring the reaction mixture in CD$_3$CN/D$_2$O = 1:4 at 100°C for 5 min. The ^{1}H NMR spectrum of **5** indicated a structure with higher symmetry, characterized by the presence of only two inequivalent ligand arms. ^{1}H DOSY NMR
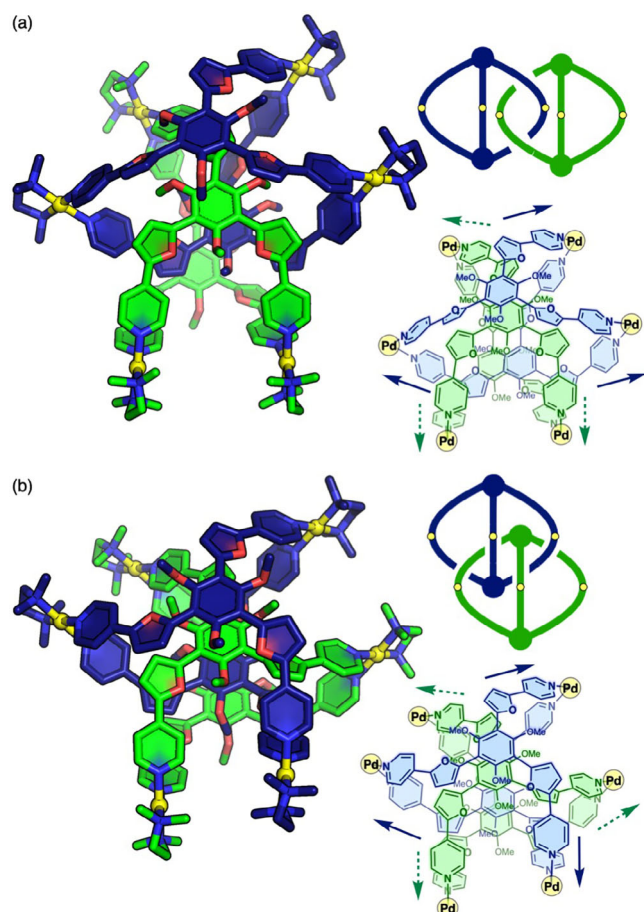
Chemistry—A European Journal | Research Article
doi.org/10.1002/chem.202500009

Chemistry
Europe
European Chemical
Societies Publishing

Figure 3. Crystal structures of (a) C_2-symmetric $(M_3L_2)_2$ **4** and (b) D_3-symmetric $(M_3L_2)_2$ **5** (carbon, mazarine or green; nitrogen, blue; oxygen, red; palladium, yellow). Hydrogen atoms, solvent molecules, and counter anions are omitted for clarity.

Figure 4. Step-by-step formation of double-walled cages through solvent changes and temperature adjustments. (i) Mixing of **2** (20 mM) and **3** (30 mM) in CD_3OD, followed by stirring at 60°C. (ii) Removal of CD_3OD in vacuo, addition of a D_2O/CD_3CN mixture (4:1 v/v), and stirring at 60°C. (iii) Heating and stirring the resulting solution at 100°C.

measurement confirmed that **5** exists as a single, well-defined product ($\log D = -9.7$, in $CD_3CN/D_2O = 1:4$, Figure S15).

A single crystal suitable for the x-ray analysis was obtained through slow anion exchange from NO_3^- to BF_4^- in acetonitrile, using CH_2I_2 as a co-crystallization agent (Figure 3b, see the Supporting Information for details).[6] Complex **5** adopts a D_3-symmetric configuration comprising two interlocked C_{3h}-symmetric M_3L_2 units.[8] As observed previously, ligand **2** forms *pseudo*-hexapodal dimeric panels via self-stacking. The averaged distances between the planes of the inner and outer benzene cores are 4.4 Å, comparable to the spacing in **1**. All four ligands in **5** adopt C_3-symmetric conformations.

We then demonstrated a one-pot, three-step conversion of self-assembled products by solvent change and temperature control (Figures 4 and S18). In the first step, ligand **2** and Pd(II) block **3** were mixed in CD_3OD (2.0 mL,[2] = 30 mM) and stirred at 60°C. After 10 min, ^1H NMR analysis revealed that [2]catenane **4** was the major product (∼80% molar ratio). Next, the solvent was removed in vacuo, and the residue was dissolved in a D_2O/CD_3CN mixture (4:1 v/v, 2.0 mL). Heating the solution at 60°C for 2 h facilitated the conversion from **4** to triply interlocked catenane **5**, with the ratio of 4:5 reaching ∼1:4. Finally, the solu-
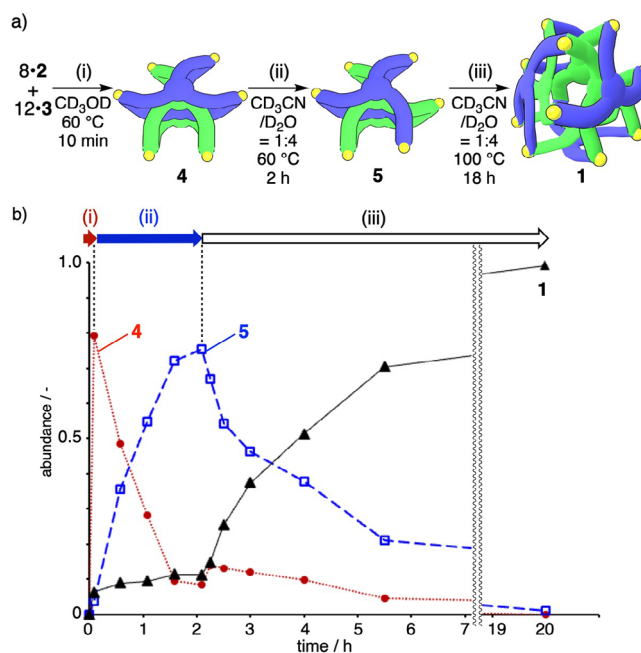
tion was heated at 100°C for an additional 18 h, resulting in the quantitative formation of double-walled cage **1**.

The observed spontaneous, multi-step transformations suggested the large differences in the formation kinetics of intermediates **4** and **5**, as well as final product **1**. In particular, intermediate **4** and **5** were formed sequentially despite their similar $(M_3L_2)_2$ interlocked structures. A simple presumption would suggest that ligand **2** adopts C_1-symmetric and C_3-symmetric conformations in a 3:1 ratio. Consequently, if there were no thermodynamic or kinetic differences in the formation of these complexes, a 3:1 mixture of **4** and **5** would be expected. However, the amount of **5** detected in the first step was consistently much smaller than predicted. This observation indicates that the formation of **4** proceeds significantly faster than that of **5**.

We hypothesized that the differences in formation kinetics are primarily influenced by the topology of the complexes.[4] The first kinetic product, complex **4**, adopts a [2]catenane structure with crossing number $n = 2$, while the second kinetic product, complex **5**, features a more intricate triply interlocked topology (ravel triply-interlocked structure) with crossing number $n = 4$.[8,9] The lower crossing number in complex **4** likely causes easy access to the structure. In contrast, the conversion from **4** to **5** is slower, partially because it requires the dissociation of at least one Pd—N(pyridyl) coordination bond, further hindering the formation of the more complex topology. Notably, ^1H NMR analysis during the conversion reveals neither isolated cage species (e.g., M_3L_2), nor fully dissociated products (such as free ligand or non-cage complexes), suggesting that these transient species are inherently unstable.

The relative thermodynamic and kinetic stability of two intermediates (**4** and **5**) and the final product **1** is assumed to increase in the order **4** < **5** < **1**. Under the tested conditions, triply-interlocked product **5** was found to be thermodynamically more stable than **4**. This conclusion was also supported by calculated formation energies (see the Supporting Information for details). The relative formation energy of **4** to **5** was estimated to be 23.8 kJ/mol in M06-2X/LanL2DZ/6-31G* level (LanL2DZ for the Pd centers) in water, modeled with the polarizable continuum model, applied to GFN2-xTB[10] optimized structures. Despite their similar double-walled structures and inter-ligand interactions, **5** exhibits more efficient inter-ligand hydrogen bonding and van der Waals contacts due to the high symmetry of its ligands and their stacking arrangement. These features are visualized in a HIGM plot[11] of the calculated structures (Figure S19). Although **5** is thermodynamically more stable than **4**, its triply interlocked topology makes it kinetically less accessible. In contrast, the final product **1**, which has the largest number of crossing points and components, benefits from extensive inter-ligand contacts that provide significant structural stabilization.

3. Conclusion

In conclusion, we succeeded in the time-resolved observations of a self-assembly process in which intermediate products underwent stepwise transformations involving topological changes, ultimately forming a double-walled knotted cage. These topological transformations represent kinetically forbidden conversions unless the reversibility of coordination bonds is considered, allowing each intermediate to possess sufficiently long residence times for isolation and enabling detailed time-resolved observation of multistep spontaneous transformations. To date, in self-assembly processes of complex structures derived from multiple chemical species, landscape models have been proposed, analogous to protein folding, where several metastable intermediate structures navigate the assembly pathways leading to the final structure. In this study, the validity of such models in self-assembly systems was demonstrated.

Furthermore, the system described in this study underscores the significance of topology in self-assembly, offering a framework to control dynamic and thermodynamic aspects. It also contributes to the understanding of why biological systems employ interlocked biomolecules such as lasso peptides[12] and knotted proteins.[13] In addition, the kinetically forbidden nature of highly interlocked topologies is a critical factor in designing dynamic systems with controllable residence times.

Conflict of Interests

The authors declare no conflict of interest.

Data Availability Statement

The data that support the findings of this study are available in the supporting information of this article.

Keywords: interlocked compound · self-assembly · topology

[1] a) K. Kinbara, T. Aida, *Chem. Rev.* **2005**, *105*, 1377; b) P. T. Corbett, J. Leclaire, L. Vial, K. R. West, J. L. Wietor, J. K. M. Sanders, S. Otto, *Chem. Rev.* **2006**, *106*, 3652; c) S. Horike, S. Shimomura, S. Kitagawa, *Nat. Chem.* **2009**, *1*, 695; d) A. Schneemann, V. Bon, I. Schwedler, I. Senkovska, S. Kaskel, R. A. Fischer, *Chem. Soc. Rev.* **2014**, *43*, 6062; e) A. J. McConnell, C. S. Wood, P. P. Neelakandan, J. R. Nitschke, *Chem. Rev.* **2015**, *115*, 7729; f) A. Stank, D. B. Kokh, J. C. Fuller, R. C. Wade, *Acc. Chem. Res.* **2016**, *49*, 809; g) W. Wang, Y.-X. Wang, H.-B. Yang, *Chem. Soc. Rev.* **2016**, *45*, 2656; h) S. Akine, *Dalton Trans.* **2021**, *50*, 4429; i) S. Akine, H. Miyake, *Coord. Chem. Rev.* **2022**, *468*, 214582.

[2] a) M. Yoneya, S. Tsuzuki, T. Yamaguchi, S. Sato, M. Fujita, *ACS Nano* **2014**, *8*, 1290; b) D. Fujita, H. Yokoyama, Y. Ueda, S. Sato, M. Fujita, *Angew. Chem., Int. Ed.* **2015**, *54*, 155; c) T. Tateishi, S. Takahashi, I. Kikuchi, K. Aratsu, H. Sato, S. Hiraoka, *Inorg. Chem.* **2021**, *60*, 16678; d) T. Abe, K. Takeuchi, M. Higashi, H. Sato, S. Hiraoka, *Nat. Commun.* **2024**, *15*, 7630.

[3] a) S. Komine, S. Takahashi, T. Kojima, H. Sato, S. Hiraoka, *J. Am. Chem. Soc.* **2019**, *141*, 3178; b) S. Hiraoka, S. Takahashi, H. Sato, *Chem. Rec.* **2021**, *21*, 443; c) D. A. Poole, III, E. O. Bobylev, S. Mathew, J. N. H. Reek, *Chem. Sci.* **2022**, *13*, 10141; d) S. Takahashi, T. Abe, H. Sato, S. Hiraoka, *Chem* **2023**, *9*, 2971; e) Z. Zhang, Z. Hu, J. Xing, Q. Li, *Responsive Mater.* **2024**, *2*, e20240009.

[4] a) J.-F. Ayme, J. E. Beves, C. J. Campbell, D. A. Leigh, *Chem. Soc. Rev.* **2013**, *42*, 1700; b) M. Frank, M. D. Johnstone, G. H. Clever, *Chem.-Eur. J.* **2016**, *22*, 14104; c) S. D. P. Fielden, D. A. Leigh, S. L. Woltering, *Angew. Chem., Int. Ed.* **2017**, *56*, 11166; d) Y. Qiu, Y. Feng, Q.-H. Guo, R. D. Astumian, J. F. Stoddart, *Chem* **2020**, *6*, 1952; e) W.-X. Gao, H.-J. Feng, B.-B. Guo, Y. Lu, G.-X. Jin, *Chem. Rev.* **2020**, *120*, 6288; f) T. Sawada, M. Fujita, *Bull. Chem. Soc. Jpn.* **2021**, *94*, 2342; g) Z. Ashbridge, S. D. P. Fielden, D. A. Leigh, L. Pirvu, F. Schaufelberger, L. Zhang, *Chem. Soc. Rev.* **2022**, *51*, 7779; h) P. Montes-Tolentino, A. S. Mikherdov, C. Drechsler, J. J. Holstein, G. H. Clever, *Angew. Chem., Int. Ed.* **2025**, *64*, e202423810.

[5] a) Y. Tamura, H. Takezawa, M. Fujita, *J. Am. Chem. Soc.* **2020**, *142*, 5504; b) Y. Tamura, H. Takezawa, M. Fujita, *Chem. Lett.* **2020**, *49*, 912.

[6] Deposition numbers 2413262 (for 4) an 2413263 (for 5) contain the supplementary crystallographic data for this paper. These data are provided free of charge by the joint Cambridge Crystallographic Data Centre and Fachinformationszentrum Karlsruhe Access Structures service.

[7] a) A. Mishra, A. Dubey, J. W. Min, H. Kim, P. J. Stang, K.-W. Chi, *Chem. Commun.* **2014**, *50*, 7542; b) L. Dang, J. Zheng, J. Zhang, T. Chen, Y. Chai, H. Fu, F. Aznarez, S. Liu, D. Li, L. Ma, *Angew. Chem., Int. Ed.* **2024**, *63*, e202406552.

[8] a) M. Fujita, N. Fujita, K. Ogura, K. Yamaguchi, *Nature* **1999**, *400*, 52; b) A. Westcott, J. Fisher, L. P. Harding, P. Rizkallah, M. J. Hardie, *J. Am. Chem. Soc.* **2008**, *130*, 2950; c) Y.-W. Zhang, S. Bai, Y.-Y. Wang, Y.-F. Han, *J. Am. Chem. Soc.* **2020**, *142*, 13614; d) Q. S. Mu, X. Y. Wang, X. Gao, G. X. Jin, *Chin. J. Chem.* **2025**, *43*, 607.

[9] a) T. Castle, M. E. Evans, S. T. Hyde, *New J. Chem.* **2008**, *32*, 1484; b) A. W. Heard, N. M. A. Speakman, J. R. Nitschke, *Nat. Chem.* **2021**, *13*, 824.

[10] a) C. Bannwarth, E. Caldeweyher, S. Ehlert, A. Hansen, P. Pracht, J. Seibert, S. Spicher, S. Grimme, *Wiley Interdiscip. Rev.:Comput. Mol. Sci.* **2021**, *11*, e1493.

[11] T. Lu, Q. Chen, *J. Comput. Chem.* **2022**, *43*, 539.

[12] a) D. F. Wyss, H.-W. Lahm, M. Manneberg, A. M. Labhardt, *J. Antibiot.* **1991**, *44*, 172; b) M. O. Maksimov, S. J. Pan, A. J. Link, *Nat. Prod. Rep.* **2012**,

Chemistry–A European Journal | Research Article
doi.org/10.1002/chem.202500009

**Chemistry
Europe**
European Chemical
Societies Publishing

29, 1909; c) J. D. Hegemann, M. Zimmermann, X. Xie, M. A. Marahiel, *Acc. Chem. Res.* **2015**, *48*, 1909.

[13] a) J. S. Richardson, *Nature* **1977**, *268*, 495; b) P. F. N. Faísca, *Comput. Struct. Biotechnol. J.* **2015**, *13*, 459; c) S.-T. D. Hsu, *Curr. Opin. Struct. Biol.* **2023**, *83*, 102709.